Archives of Biochemistry and Biophysics 637 (2018) 73–78

Contents lists available at ScienceDirect

Archives of Biochemistry and Biophysics

journal homepage: www.elsevier.com/locate/yabbi

Understanding the molecular basis of the high oxygen affinity variant human hemoglobin Coimbra

S.E. Jorge[a], M. Bringas[b,c], A.A. Petruk[b,c], M. Arrar[b,c], M.A. Marti[d,e], M.S. Skaf[f], F.F. Costa[g], L. Capece[b,c], M.F. Sonati[a], D. Estrin[b,c,*]

[a] Department of Clinical Pathology, School of Medical Sciences, University of Campinas (Unicamp), Campinas, SP, Brazil
[b] Universidad de Buenos Aires, Facultad de Ciencias Exactas y Naturales, Departamento de Química Inorganica, Analítica y Química-Física, Buenos Aires, Argentina
[c] CONICET-Universidad de Buenos Aires, Instituto de Quimica Física de los Materiales, Medio Ambiente y Energía (INQUIMAE), Buenos Aires, Argentina
[d] Universidad de Buenos Aires, Facultad de Ciencias Exactas y Naturales, Departamento de Química Biológica, Buenos Aires, Argentina
[e] CONICET-Universidad de Buenos Aires, Instituto de Química Biológica de la Facultad de Ciencias Exactas y Naturales (IQUIBICEN), Buenos Aires, Argentina
[f] Institute of Chemistry, State University of Campinas (Unicamp), Campinas, SP, Brazil
[g] Hematology and Hemotherapy Center, University of Campinas (Unicamp), Campinas, SP, Brazil

ARTICLE INFO

Keywords:
Hemoglobin variant
Hb Coimbra
Allostery
Oxygen affinity
Polycythemia

ABSTRACT

Human hemoglobin (Hb) Coimbra (βAsp99Glu) is one of the seven βAsp99 Hb variants described to date. All βAsp99 substitutions result in increased affinity for O_2 and decreased heme-heme cooperativity and their carriers are clinically characterized by erythrocytocis, caused by tissue hypoxia. Since βAsp99 plays an important role in the allosteric α1β2 interface and the mutation in Hb Coimbra only represents the insertion of a CH_2 group in this interface, the present study of Hb Coimbra is important for a better understanding of the global impact of small modifications in this allosteric interface. We carried out functional, kinetic and dynamic characterization of this hemoglobin, focusing on the interpretation of these results in the context of a growth of the position 99 side chain length in the α1β2 interface. Oxygen affinity was evaluated by measuring p50 values in distinct pHs (Bohr effect), and the heme-heme cooperativity was analyzed by determining the Hill coefficient (*n*), in addition to the effect of the allosteric effectors inositol hexaphosphate (IHP) and 2,3-bisphosphoglyceric acid (2,3-BPG). Computer simulations revealed a stabilization of the R state in the Coimbra variant with respect to the wild type, and consistently, the T-to-R quaternary transition was observed on the nanosecond time scale of classical molecular dynamics simulations.

1. Introduction

Human hemoglobin (Hb) is the hemeprotein found in high concentrations in erythrocytes, and is functionally responsible for the transport of oxygen (O_2) from the lungs to peripheral tissues. Hb is a tetramer comprised of two α-like (α or ζ) and two β-like (β, δ, γ or ε) globin chains, each associated with a *heme* group, a protoporphyrin IX with a ferrous iron atom that can reversibly bind molecular O_2. The different combinations of globin chains are adapted to distinct stages of human development from the embryonic period to adult life, depending on the O_2 demand and environmental availability. During fetal life, for example, fetal hemoglobin (HbF) (α2β2), a variant that has high affinity for O_2, due to its decreased affinity for the allosteric effector 2,3-biphosphoglycerate (2,3-BPG), is expressed to compete for the O_2 from maternal HbA (α2β2), which is mainly produced during adult life [1].

The stability of the tetramer is controlled by the α1β1/α2β2 contacts, whereas the α1β2/α2β1 interface ensures the stability of the transition between the two conformations with different oxygen affinity, known as the T (Tense) and R (Relaxed) states, with low and high affinity for O_2, respectively [2,3]. The α1β2 interface is particularly close to the heme pocket, such that changes in this interface are closely related to O_2 binding. One of the most important interactions in the α1β2 interface involves βAsp99, which forms hydrogen bonds with αTyr42 and αAsn97, stabilizing the T state (Fig. 1) [2,4].

Until now, 99 human Hb variants with high oxygen affinity have been reported, and 79 of them involve β-chain residue replacements. The majority of these variants have substitutions at one of the three crucial regions for Hb stability and function: the β-chain C terminus, the α1β2 interface and the 2,3-BPG binding site. To date, seven hemoglobin βAsp99 substitution variants have been detected: Hb Ypsilanti

* Corresponding author. Universidad de Buenos Aires, Facultad de Ciencias Exactas y Naturales, Departamento de Química Inorganica, Analítica y Química-Física, Buenos Aires, Argentina.
E-mail address: dario@qi.fcen.uba.ar (D. Estrin).

https://doi.org/10.1016/j.abb.2017.11.010
Received 5 July 2017; Received in revised form 21 November 2017; Accepted 22 November 2017
Available online 01 December 2017
0003-9861/

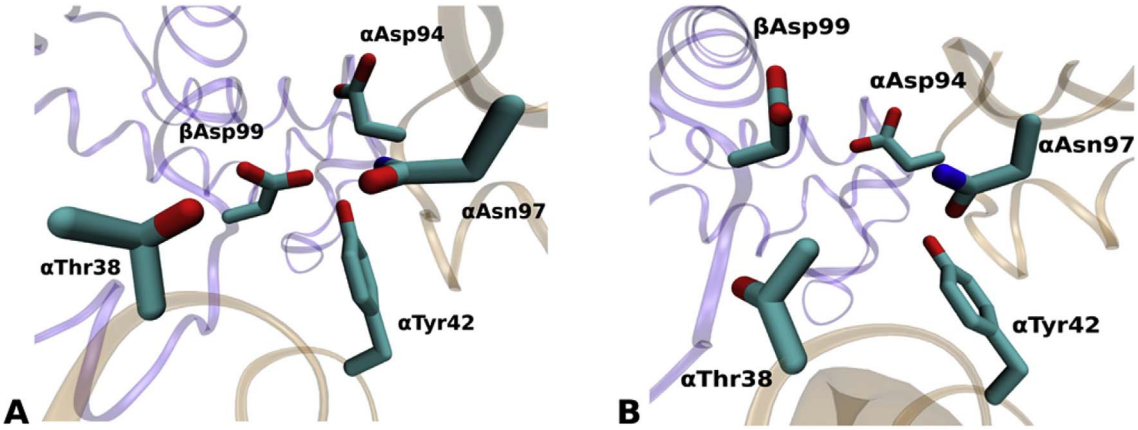

Fig. 1. The α1β2 Hb interface; α1 in orange and β2 in purple. βD99 interactions in the (A) HbA deoxy, or T state (PDB ID 2HHB), and (B) the oxy, or R state (PDB ID 1HHO). (For interpretation of the references to colour in this figure legend, the reader is referred to the web version of this article.)

(βAsp99Tyr), Hb Kempsey (βAsp99Asn), Hb Yakima (βAsp99His), Hb Radcliffe (βAsp99Ala), Hb Hotel-Dieu (βAsp99Gly) and Hb Coimbra (βAsp99Glu). In all these cases, substitution of βAsp99 resulted in increased O_2 affinity and a decreased heme-heme cooperativity. Moreover, individuals with any of these mutations, in heterozygosis, are clinically characterized by erythrocytosis [5]. The mechanism of this compensatory production of red blood cells (also known as polycythemia), mediated by the presence of these hemoglobin variants is, therefore, caused by tissue hypoxia that prompts higher levels of erythropoietin and consequently intensive erythropoiesis [1,6–8].

It is interesting that these deleterious mutations can be as subtle as that of the Asp99Glu mutation in Hb Coimbra, and still significantly affect Hb function. The difference between HbA and Hb Coimbra is, at a molecular level, the insertion of a methylene group in the α1β2 interface. Nevertheless, this variant is characterized by an increased affinity for O_2 and subsequent erythrocytosis, as well as other clinical complications caused by the hyperviscosity of the blood in its carriers. The study of Hb Coimbra is, therefore, key to a better understanding of the underlying mechanisms of the T-to-R transition [9,10], because it is an example of how a small change in the α1β2 interface can have a dramatic impact on protein function.

2. Materials and methods

The samples studied here were obtained from peripheral blood of three carriers of Hb Coimbra, who were referred to the Hematology and Hemotherapy Center, University of Campinas, in Campinas, State of São Paulo, Brazil, for investigation of hemoglobinopathies. Ethical aspects and inform consent involved in this project were approved by the Brazilian research ethics committee (CAAE.0036.0146.000–07; Project 061/2007). The results obtained here were compared to six control samples: three samples collected from adults, mainly containing HbA; three samples from newborn individuals, mainly composed of HbF).

The erythrocytes were isolated, washed in cold saline and the Hb content were extracted by lysis in deionized water and the debris were removed by centrifuging.

2.1. Functional assays

Oximetry tests at pH 7.4 were carried out in a Hemox Analyzer system (TCS Scientific Corporation, New Hope, PA, USA) using 25 ⌈L of red blood cell concentrate, stored at −80 °C, and following the standard protocol and reagents recommended by the manufacturer (TCS Scientific Corporation). The results of oxygen affinity and heme-heme cooperativity of the Hb Coimbra in the lysates (containing Hb Coimbra, HbA, as well as HbA_2 – approximately 2.5%, and HbF – approximately 1%), were compared to three standard hemolysate mainly containing HbA (95%), as well as three newborn erythrocytes lysates (with levels of HbF varying from 63.8% to 87.4%). No protein purification was performed for these analyses and all samples were treated and stored under the same conditions and period.

The function of Hb Coimbra from cell lysates were also studied after purification with Sephadex G-25 gel chromatography (Sigma–Aldrich, St. Louis, MO, US), at pH 8.2 and pH 6.2, in Hepes buffer (*N*-(2Hydroxyethyl) piperazine-*N*′-2-ethane sulfonic acid) buffer– 50 mM (Sigma–Aldrich, St. Louis, MO, US), without addition of NaCl. In order to guarantee the elimination of 2,3-BPG and other organic phosphates from the samples, an Amberlite Mixed Bed column (MB 150; Sigma–Aldrich, St. Louis, MO, US) was also used. Hb and globin chain integrity was verified by Native-PAGE and SDS-PAGE (data not shown). The stripped lysates (Hb concentration of 70 ⌈M/heme) were submitted to spectrophotometric method at 25 °C, pH range 6.5–8.5, as previously described by Rossi-Fanelli and Antonini [2,11]. The equilibrium curves were performed in the absence and the presence of inositol hexaphosphate (IHP, 1 mM) (Sigma–Aldrich, St. Louis, MO, US). Sigmoidal fitting was performed using OriginPro 8.0. Oxygen affinity (determined by p50), Bohr effect and heme-heme cooperativity (determined by the Hill coefficient) from the lysates with Hb Coimbra were compared to stripped lysate mainly containing HbA [2,11,12]. The O_2 affinity of Hb Coimbra was also determined under the influence of 2,3-Biphosphoglyceric acid (2,3-BPG, 1 mM) (2,3-Biphospho-D-glyceric acid pentasodium; Sigma–Aldrich, St. Louis, MO, US), pH 7.6, 25 °C, and compared to that of HbF and HbA, from newborn and adult stripped samples, respectively.

2.2. Kinetics

Kinetic studies were performed using stopped-flow spectrophotometry in a stopped flow module SFM-300 (Bio-Logic Science Instruments, Seyssinet-Pariset, France) and the UV–vis traces were recorded using the Bio-kine 32 software (Bio-Logic Science Instruments). An integration time of 0.8 ms was used for all measurements (monitoring Hb-O_2 dissociation and Hb-CO ligation in the range of 400–700 nm), at 25 °C. Hb concentration (from stripped hemolysate) used here was 80 μM/heme in 100 mM phosphate buffer (J. T. Baker – Fisher Scientific, Pittsburg, PA, US), adjusted to pH 7.4. The dissociation rate constant k_{off} was obtained from the reaction of Hb with Sodium dithionite (DTS - Sigma–Aldrich, St. Louis, MO, US) 6 mM, as reducing agent [13–15], in the ratio of 1:3 (Hb:DTS). Absorbance at 430 nm (absorbance maxima of the deoxi-Hb in the Soret region) as a function of time was used, and the kinetic trace was adjusted monoexponentially, to obtain one characteristic unimolecular constant for the process (Table 2). The same experimental conditions were used to determine k_{off} in presence of 1 mM IHP (Sigma–Aldrich, St. Louis, MO,

US). Two distinct samples of Hb Coimbra were used for this experiment (20 measurements each) and the results were compared to kinetic traces obtained from the reaction of two control samples of HbA with DTS (20 measurements each).

The constant of ligation of Hb-CO was obtained from the reaction between reduced Hb (80 ⌈M/heme) by DTS (6 mM) in 100 mM phosphate buffer saturated with CO. To achieve saturation, the solution was exposed to carbon monoxide (CO) produced from a mixture of formic and sulfuric acid at low temperature for 1 h. A pseudo first order rate was obtained, and then corrected using the tabulated CO solubility at 25 °C to retrieve a second order rate. The reaction ratio was 1:5 [ferrous Hb: phosphate buffer saturated with CO]. Five measurements from two distinct samples of Hb Coimbra were obtained and the results were compared to two control samples of HbA (5 measurements each).

2.3. Molecular dynamics (MD) simulations

All simulations were performed using the Amber14 software package. The ff99SB force field [16] was used for the polypeptide chains and the TIP3P water model [17] for the solvent. The heme group parameters were generated and widely tested in our group, for both R and T states [10,18–21]. The tetrameric protein was solvated in a 36 Å truncated octahedron. Periodic boundary conditions were used and a cutoff of 12 Å for van der Waals interactions. A time-step of 2.0 fs was used, keeping bonds to hydrogen atoms rigid using the SHAKE algorithm [22]. The total charge of the system was neutralized using Amber's uniformly charged plasma. A standard protocol for heating and equilibration was used, consisting of a slow heating of 500 ps from 0 to 300K was carried out, followed by 200 ps of NPT molecular dynamics, to achieve a reasonable density of the system. Finally, a 200-ns production MD was performed in NVT conditions. The Berendsen thermostat and barostat were used to control the system temperature and pressure, respectively [23].

Since there are no crystallographic structures of hemoglobin Coimbra, all simulated Coimbra systems refer to *in silico* mutations of wild type adult human hemoglobin structures. We performed molecular dynamics simulations of the Hb tetramers starting from the R (oxy) and T (deoxy) X-ray structures of the wild type HbA to check if the simulations were able to maintain their respective quaternary states, and avoid spontaneous T-to-R transitions [24]. PDB structures 1HHO [25] and 2HHB [26] were chosen as initial structures for the simulations of the R and T states, respectively.

Four deoxy systems were simulated. Two of them, wild type and the βAsp99Glu *in silico* mutant, were started from the crystallographic structure in the T state: WT-XR and Coimbra-XR, respectively. After 200 ns MD of the XR systems, each of these was mutated in the β99 position (wt to βAsp99Glu and vice versa), generating two new structures which will be referred as Coimbra-MD and WT-MD. Three replicas of each of these systems were simulated. The essential mode that connects the T and R quaternary states was calculated [27] using principal component analysis of the two wild type crystallographic tetrameric structures; we refer to these modes as the T-to-R quaternary transition mode. The 200 ns MD trajectories were later projected onto these essential modes to characterize the conformational states.

Two conformational parameters were also monitored to evaluate the T-to-R quaternary state transition: the α1-β2 and α2-β1 angle, which is known to be an indicator of the quaternary state of the tetramer, and the αThr38-βHis97 distance, which is a relevant magnitude associated with the hinge region. In addition, the Cα -Cβ -Cδ angle of the β99 side chain, an indicator of whether the residue is pointing towards the neighbouring α subunit or not, was considered.

The ΔΔG of the T-to-R transition due to the βAsp99Glu mutation was estimated using a thermodynamic cycle that connects the R and T quaternary states in wild type and Coimbra variants. ΔG for both mutations in each state was calculated using an alchemical free energy transformation [28,29], in which a coupling parameter λ, with values between 0 and 1 corresponding to the wild type and Asp99Glu states, respectively, was introduced into the classical Hamiltonian. To enhance the sampling across λ-space, the adaptive integration method (AIM) implemented in the PMEMD module of Amber was used [30], in which a single trajectory attempts Monte Carlo changes in its value of λ. Twelve values for λ were used for the *in silico* mutation: [0, 0.05, 0.1, 0.2, 0.3, 0.4, 0.5, 0.6, 0.7, 0.8, 0.9, 0.95, 1] and the multi-state Bennett Acceptance Ratio [31] estimator was used to estimate the ΔG values. Both the number of roundtrips in λ space, as well as the time-evolution of the ΔG estimate, were taken into account in assessing the convergence of the free energy calculations.

3. Results

3.1. Functional assays

Functional assays by oximetry performed with unpurified erythrocyte lysate, at pH 7.4 and temperature of 37 °C, close to the physiological conditions, indicate that the O_2 affinity of Hb Coimbra is greater than that of adult hemoglobin (HbA) and that of fetal hemoglobin (HbF) from newborn samples with levels of HbF of 68.3–87.4%. The unpurified samples of Hb Coimbra also demonstrated higher affinity in comparison to samples with 100% of HbF, which is known to have very high oxygen affinity because of its decreased affinity for 2,3-BPG (Table 1 and Fig. 2).

The Asp99Glu variant had the same behavior in both O_2-dissociation (Fig. 2A) and O_2-association curves (Fig. 2B), with a consistently lower p50 value than HbA and newborn hemolysate. As expected, the Hill coefficient (n) indicated decreased heme-heme cooperativity (Table 1).

In agreement with the oximetry functional assays, tonometry-spectrophotometry experiments with stripped lysate also demonstrated increased affinity for oxygen, even in the presence of allosteric effector 2,3-BPG (1 mM), in 50 mM Hepes buffer, pH 7.5, 25 °C (Fig. 3).

Under these conditions, the stripped hemolysates containing mainly HbF had a lower O_2 affinity than adult Hb (Fig. 3A). On the other hand, in the presence of 2,3-BPG, HbF had higher O_2 affinity than HbA, because of its known lower affinity for 2,3-BPG. In contrast, Hb Coimbra demonstrated higher O_2 affinity than both HbA and HbF hemolysates, regardless of the presence of 2,3-BPG.

Consistent with the experiments performed with unpurified lysates containing the HbA variant, the Hill coefficient for stripped Hb Coimbra was also decreased in comparison to controls ($n_{Hb\ Coimbra} = 1.29 \pm 0.12$; $n_{Hb\ A} = 2.0 \pm 0.01$; $n_{Hb\ F} = 2.2 \pm 0.05$). In the presence of 2,3-BPG, the Hill coefficient was slightly increased, however still lower than those of HbA and HbF ($n_{Hb\ Coimbra} = 1.45 \pm 0.13$; $n_{HbA} = 2.0 \pm 0.08$; $n_{HbF} = 1.73 \pm 0.15$).

This behavior was also confirmed in the pH range 6.5–8.5, at 25 °C, in stripped condition (Fig. 4).

We further evaluated the allosteric effect of IHP, an organic phosphate that presumably occupies the same 2,3-BPG site in human Hb, decreasing its O_2 affinity [32], in the same pH range of 6.5–8.5, at 25 °C. In both wild type and Hb Coimbra, the O_2 affinity tends to decrease in the presence of IHP (Fig. 4). Regarding the Bohr effect, no

Table 1
p50 values and Hill coefficients (n) for O_2 saturation and dissociation, measured for HbF, HbA and Coimbra variants from unpurified cell lysates.

		p50 (mmHg)	Hill coefficient (n)
HbA (~ 95%)	dissociation	15.56 ± 0.50	2.51 ± 0.18
	saturation	15.56 ± 0.77	2.41 ± 0.22
HbF (~ 77%)	dissociation	10.03 ± 0.58	2.25 ± 0.16
	saturation	11.41 ± 0.77	1.77 ± 0.36
Hb Coimbra	dissociation	7.94 ± 0.69	1.46 ± 0.06
	saturation	7.60 ± 1.06	1.38 ± 0.15

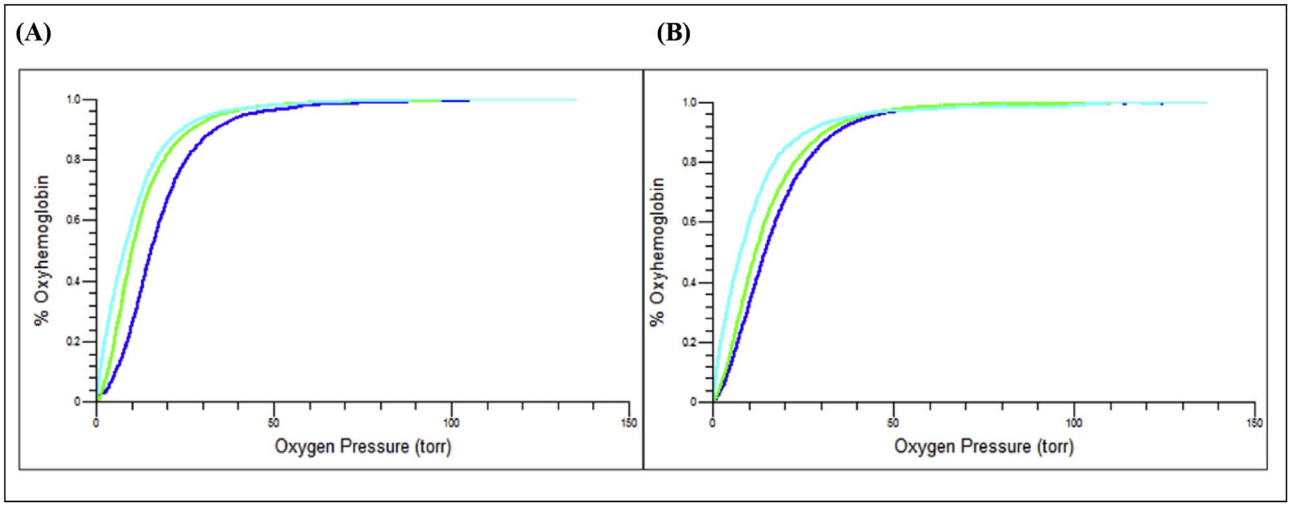

Fig. 2. Equilibrium curves of the unpurified hemolysates. Dissociation **(A)** and saturation **(B)** curves for Hb-O_2 for lysates containing mainly HbA (blue), HbF (green) and Hb Coimbra (cyan). (For interpretation of the references to colour in this figure legend, the reader is referred to the web version of this article.)

significant difference was observed in comparison to HbA, under the analytical conditions analyzed here (Fig. 4).

3.2. Kinetics

Despite the low heme-heme cooperativity in Hb Coimbra, we found that the dissociation rate constant k_{off} Hb-O_2 was not significantly different between HbA and Hb Coimbra (Table 2). We also found that the presence of IHP (1 mM) decreases the O_2 dissociation rate more so in stripped Hb Coimbra than in wild type Hb A (Table 2).

Using CO as a molecular probe, we compared the association rate kinetics for both hemoglobins and found that the k_{on} CO value for Hb Coimbra was much higher than that of the wild type, indicating a facilitated T-to-R displacement in Hb Coimbra that favors the R state (Table 2).

3.3. MD simulations

After adequate equilibration, the deoxy state of both HbA and Hb Coimbra was simulated for 200 ns in triplicate, beginning from either the crystallized T state or an MD conformation, as described in the

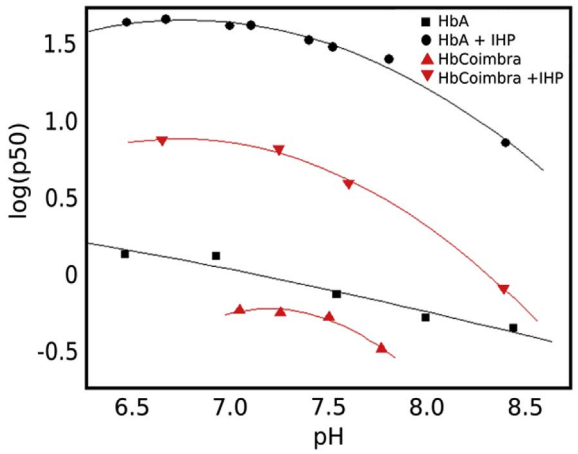

Fig. 4. Bohr Effect of Hb Coimbra hemolysate in comparison with that of wild type HbA, demonstrating the partial affinity of the Hb variant [log(p50)], in the presence and absence of IHP (1 mM). Curves represent second-order polynomial fits of the data.

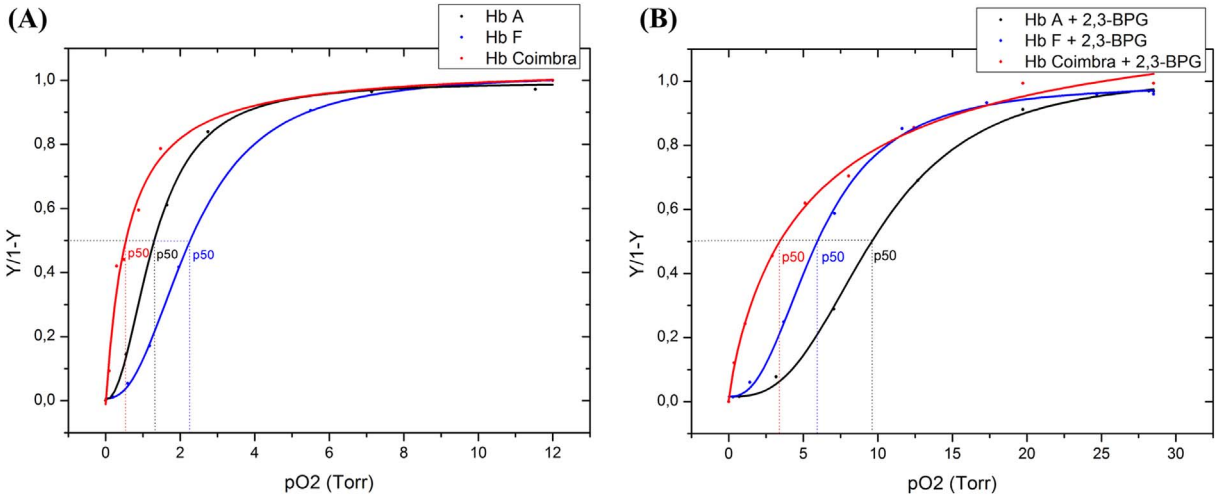

Fig. 3. Equilibrium curves of stripped hemolysates containing mainly HbA (black), HbF (blue), and Hb Coimbra (red) in the absence **(A)** and in the presence **(B)** of 2,3-BPG (1 mM). Curves represent sigmoidal fits of the data. (For interpretation of the references to colour in this figure legend, the reader is referred to the web version of this article.)

Table 2
Values of dissociation rate constants (k_{off}) of Hb Coimbra- O_2 in absence and presence of IHP and association rate constants of Hb Coimbra-CO (k_{on}CO), determined by Stopped Flow experiments.

	k_{off} (s^{-1})	k_{off} (+IHP) (s^{-1})	k_{on} CO (s^{-1} M^{-1})
Hb A	39 ± 2	35.7 ± 0.6	94.73 ± 0.02
Hb Coimbra	38 ± 1	25.8 ± 0.4	160.72 ± 0.02

Methods section. The time evolution of the root mean square deviation (RMSD) from the initial structure was analyzed as an indication of the conformational stability. Whereas both wild type systems remained stable during the MD simulations, both Coimbra-XR and -MD systems showed an increase in RMSD at approximately 20 ns.

To assess whether the large RMSD observed in the simulations of Hb Coimbra was due to a quaternary structural transition, we calculated the angle between the αβ heterodimers of each system and compared to that of deoxy HbA after structurally aligning the α1 and β1 monomers (Fig. 5A) [21,33]. We also monitored the distance between Cα atoms of αThr41 and βHis97, residues located in the switch region. Both Coimbra systems (XR and WT) showed an increase in the αThr41Cα -βHis97Cα distance (Fig. 5B).

We calculated the quaternary T-to-R transition essential modes between the 2HHB to 1HHO crystallographic structures, as described in the Methods. We then projected the structures from the MD trajectories onto these modes to classify the conformational state during the simulations. In Fig. 6 the projection of all four systems onto the first T-to-R quaternary transition mode is shown.

We expected that the WT-MD system would not return from the R to the T state in the time scale of the simulation. This process is expected to happen on the order of 20 μs, even though a direct time-scale comparison should not be made between simulated time and experimental measurements. Our results show that the Coimbra-XR and -MD systems undergo the T-to-R transition in 10–20 ns, whereas the wild type simulations remain in their initial conformational states. This rapid conversion in Hb from the T state to the R state, inducing a large-scale conformational change, in Hb Coimbra is consistent with the preference of the variant for the R conformation suggested by the experiments.

Due to the efficient packing of βD99 in the deoxy and not in the oxy state (Fig. 1), we did not expect a significant effect of the βAsp99Glu replacement on the simulation time scale of HbA Coimbra. To further investigate the thermodynamic basis of the enhanced quaternary T-to-R transition observed in simulations of HbA Coimbra, we computed the

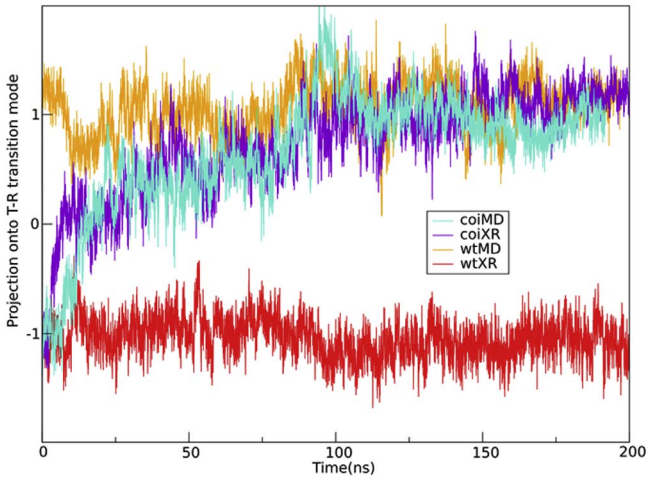

Fig. 6. WT-XR system structures projected on the T to R transition mode. The value −1 corresponds to the T state and the value 1, to the R state.

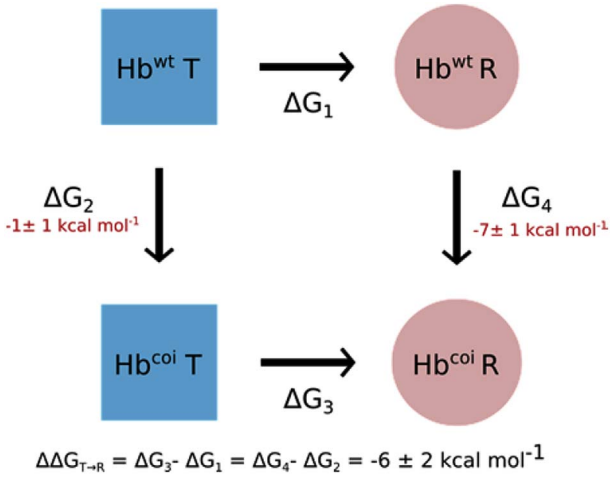

Fig. 7. Thermodynamic cycle for the T-to-R transition in wild type and Coimbra Hb. Free energies reported are averages of four independent trials, two replicates for each of the β1 and the β2 subunits. Error was estimated using the standard deviation of the four values.

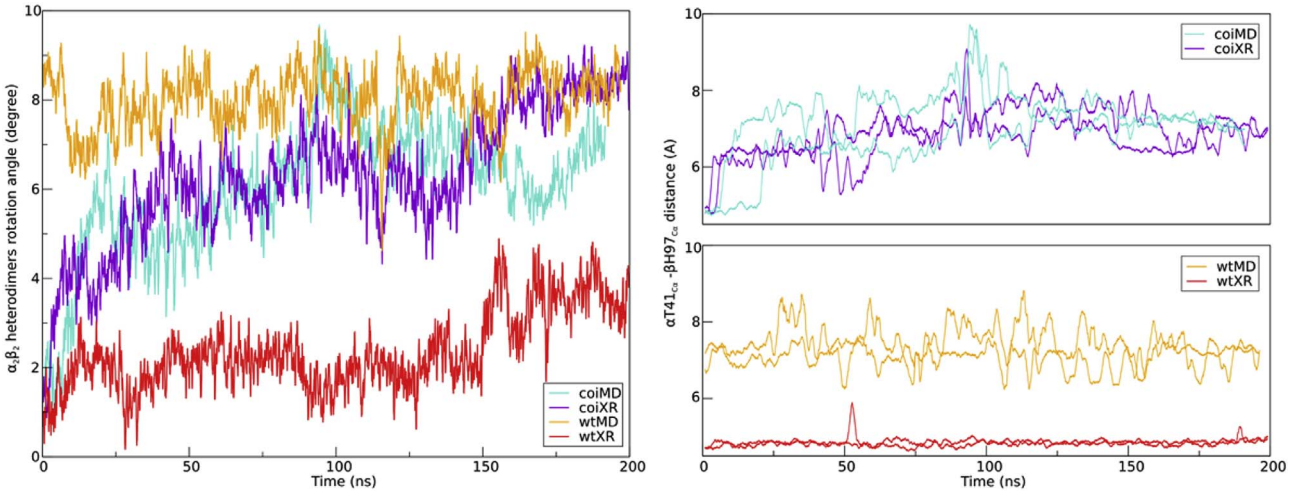

Fig. 5. α_2-β_2 rotation angle vs time for the simulated systems: wt-XR, wt-MD, Coimbra-XR and Coimbra-MD (left) and αT41C_α -βT97C_α distance (right) for both $\alpha_1\beta_2$ and $\alpha_2\beta_1$.

ΔΔG of the T-to-R transition as the result of the βAsp99Glu substitution, as illustrated in the thermodynamic cycle in Fig. 7. Specifically, we performed the alchemical transformations corresponding to the βAsp99Glu replacement in both T and R conformational states; i.e, ΔG_1 and ΔG_2 in Fig. 7. We found that the mutation favors the T-to-R transition by approximately 6 kcal/mol, and this bias is indeed due to a stabilization of the R state as the result of D99E substitution, whereas the T state is unaffected by the mutation. This is consistent with the observed T-to-R transition in the short time scale of the unbiased MD simulation.

4. Discussion and conclusion

Our results indicate that Hb Coimbra consistently has very high affinity for O_2 than wild type HbA and HbF, in the percentages found in human hemolysates. Decreased p50 values were found in all different conditions studied here: samples without purification/desalinization treatment, samples stripped and studied in the absence and presence of allosteric effectors 2,3-BPG and IHP, and in a range of pH values from 6.5 to 8.5. No differences in Bohr effect were found.

Though k_{off} values of Hb Coimbra and HbA show no difference in intrinsic O_2 affinity resulting from local changes close to the heme moiety, our results demonstrate that the favored T-to-R transition in Hb Coimbra coincides with an increase in the k_{on}. The underlying cause of the differences observed in Hb Coimbra appear to be allosteric in nature. Indeed, the experiments performed both in presence and absence of the allosteric effectors 2,3 BPG and IHP clearly show that the Asp99Glu substitution decreases heme-heme cooperativity.

Projection of the MD simulations onto the transitional essential mode allowed us to follow the conformational state of the tetramer. MD simulations of the deoxy structures of the *in silico* variant showed a facilitated transition from the T to the R state, whereas the HbA structures remained in their initial quaternary states on the time scales of our simulations.

Free energy calculations confirmed a preference of Hb Coimbra for the R state. This fact can be interpreted from a molecular point of view in terms of the α1β2 interactions. Hydrogen bonding at this interface is crucial in stabilizing the quaternary state, and the steric hindrance due to the longer chain of aspartate than that of glutamate modifies the free energy hypersurface in the quaternary transition path.

The inter-chain interactions present in the αβ interfaces play an important role in the relative stability of the T and R states. In this case, the disruption of hydrogen bonds in this region in the T state resulted in a thermodynamic preference for the R conformation, a fact that is experimentally supported by a decreased p50 value. Evidence from the measured kinetic rate constants are also in agreement, with an increased k_{on} CO value with respect to wild type HbA, and an IHP-induced decrease in the k_{off} value revealing the tendency of Hb Coimbra to shift from the T towards the R state.

Taken together, our computational and experimental results point to the fact that the observed pathological effects related to the presence of the Hb Coimbra replacement are due to the alteration of the T-to-R transition thermodynamics, promoted by a subtle change of the intermolecular interactions responsible for the stabilization of the quaternary structure.

Acknowledgments

This work was supported by São Paulo Research Foundation (Fapesp, Fellowship 2015/13710–1, Grants 2014/00984-3), National Council for Research (CNPq)/Brazil (306675/2013-7), as well as Universidad de Buenos Aires Grants UBA-CyT 20020130100097BA, ANPCYT PICT 2014-1022 (to D.A.E).

M.A was supported in part by an NSF postdoctoral fellowship in biology (Award number 1401889).

References

[1] V. Hoffbrand, J.E. Pettit, P.A.H. Moss, Essential Haematology, 4.ed, Blackwell Science, London, Edinburgh, Boston, 2000, p. 437.
[2] E. Antonini, M. Brunori, Hemoglobin and Myoglobin in Their Reaction with Ligands, North-Holland Publishing Company, Amsterdam, 1971, p. 435 (v.21).
[3] R.M. Esquerra, B.M. Bibi, P. Tipgunlakant, I. Birukou, J. Soman, J.S. Olson, D.S. Kliger, R.A. Goldbeck, Role of heme pocket water in allosteric regulation of ligand reactivity in human hemoglobin, Biochemistry 55 (29) (2016) 4005–4017.
[4] H.-W. Kim, T.-J. Shen, D.P. Sun, N.T. Ho, M. Madrid, M.F. Tam, M. Zou, P.F. Cottam, C. Ho, Restoring allosterism with compensatory mutations in hemoglobin, Proc. Natl. Acad. Sci. 91 (24) (1994) 11547–11551.
[5] Globin Gene Server Home Page. (http://globin.cse.psu.edu). Last accessed on 21 June 2017.
[6] H. Wajcman, F. Galacteros, Hemoglobins with high oxygen affinity leading to erythrocytosis, new Var. new concepts, Hemoglobin 29 (2) (2005) 91–106.
[7] V.R. Gordeuk, D.W. Stockton, J.T. Prchal, Congenital polycythemias/erythrocytoses, Haematologica 90 (1) (2005) 109–116.
[8] F.G. Fernández, A. De Francisco, A.C. Gomez, J. Ruiz, E. Rodrigo, M. Arias, The phenomenon of hemoglobin variability with erythropoiesis stimulating agents in renal transplant patients, Clin. Nephrol. 72 (4) (2009) 292–297.
[9] W.A. Eaton, E.R. Henry, J. Hofrichter, A. Mozzarelli, Is cooperative oxygen binding by hemoglobin really understood? Nat. Struct. Mol. Biol. 6 (4) (1999) 351–358.
[10] W.A. Eaton, E.R. Henry, J. Hofrichter, S. Bettati, C. Viappiani, A. Mozzarelli, Evolution of allosteric models for hemoglobin, IUBMB life 59 (8–9) (2007) 586–599.
[11] A. Rossi-Fanelli, E. Antonini, Studies on the oxygen and carbon monoxide equilibria of human myoglobin, Archives Biochem. Biophysics 77 (2) (1958) 478–492.
[12] I. Binotti, S. Giovenco, B. Giardina, E. Antonini, M. Brunori, J. Wyman, Studies on the functional properties of fish hemoglobins: Ii. the oxygen equilibrium of the isolated hemoglobin components from trout blood, Archives Biochem. Biophysics 142 (1) (1971) 274–280.
[13] K. Vandegriff, J. Olson, The kinetics of O2 release by human red blood cells in the presence of external sodium dithionite, J. Biol. Chem. 259 (20) (1984) 12609–12618.
[14] J.P. Harrington, D. Elbaum, R.M. Bookchin, J.B. Wittenberg, R.L. Nagel, Ligand kinetics of hemoglobin s containing erythrocytes, Proceedings of the National Academy of Sciences 74 (1) (1977) 203–206.
[15] T. Brittain, R. Simpson, An analysis of the stopped-flow kinetics of gaseous ligand uptake and release by adult mouse erythrocytes, Biochem. J. 260 (1) (1989) 171–176.
[16] K. Lindorff-Larsen, S. Piana, K. Palmo, P. Maragakis, J.L. Klepeis, R.O. Dror, D.E. Shaw, Improved side-chain torsion potentials for the amber ff99sb protein force field, Proteins Struct. Funct. Bioinforma. 78 (8) (2010) 1950–1958.
[17] W.L. Jorgensen, J. Chandrasekhar, J.D. Madura, R.W. Impey, M.L. Klein, Comparison of simple potential functions for simulating liquid water, J. Chem. Phys. 79 (2) (1983) 926–935.
[18] M.A. Marti, A. Crespo, L. Capece, L. Boechi, D.E. Bikiel, D.A. Scherlis, D.A. Estrin, Dioxygen affinity in heme proteins investigated by computer simulation, J. Inorg. Biochem. 100 (4) (2006) 761–770.
[19] A. Bidon-Chanal, M. Martí, D. Estrin, F. Luque, Exploring the nitric oxide detoxification mechanism of mycobacterium tuberculosis truncated haemoglobin n, SelfOrganization of Molecular Systems, Springer, 2009, pp. 33–47.
[20] A.D. Nadra, M.A. Martí, A. Pesce, M. Bolognesi, D.A. Estrin, Exploring the molecular basis of heme coordination in human neuroglobin, Proteins Struct. Funct. Bioinforma. 71 (2) (2008) 695–705.
[21] L. Capece, D.A. Estrin, M.A. Marti, Dynamical characterization of the heme no oxygen binding (hnox) domain, Insight into soluble guanylate cyclase allosteric transit. Biochem. 47 (36) (2008) 9416–9427.
[22] J.-P. Ryckaert, G. Ciccotti, H.J. Berendsen, Numerical integration of the cartesian equations of motion of a system with constraints: molecular dynamics of n-alkanes, J. Comput. Phys. 23 (3) (1977) 327–341.
[23] H.J. Berendsen, J.P.M. Postma, W.F. van Gunsteren, A. DiNola, J. Haak, Molecular dynamics with coupling to an external bath, J. Chem. Phys. 81 (8) (1984) 3684–3690.
[24] J.S. Hub, M.B. Kubitzki, B.L. De Groot, Spontaneous quaternary and tertiary T-R transitions of human hemoglobin in molecular dynamics simulation, PLoS Comput. Biol. 6 (5) (2010) e1000774.
[25] B. Shanaan, Structure of human oxyhaemoglobin at 2.1 A resolution, J. Mol. Biol. 171 (1983) 31–59.
[26] G. Fermi, M. Perutz, B. Shaanan, R. Fourme, The crystal structure of human deoxyhaemoglobin at 1.74 A resolution, J. Mol. Biol. 175 (2) (1984) 159–174.
[27] A. Amadei, A. Linssen, H.J. Berendsen, Essential dynamics of proteins, Proteins Struct. Funct. Bioinforma. 17 (4) (1993) 412–425.
[28] J.G. Kirkwood, Statistical mechanics of fluid mixtures, J. Chem. Phys. 3 (5) (1935) 300–313.
[29] R.W. Zwanzig, High-temperature equation of state by a perturbation method. i. nonpolar gases, J. Chem. Phys. 22 (8) (1954) 1420–1426.
[30] J.W. Kaus, M. Arrar, J.A. McCammon, Accelerated adaptive integration method, J. Phys. Chem. B 118 (19) (2014) 5109–5118.
[31] M.R. Shirts, J.D. Chodera, Statistically optimal analysis of samples from multiple equilibrium states, J. Chem. Phys. 129 (12) (2008) 124105.
[32] R. Edalji, R.E. Benesch, R. Benesch, Binding of inositol hexaphosphate to deoxyhemoglobin, J. Biol. Chem. 251 (23) (1976) 7720–7721.
[33] S. Fischer, K.W. Olsen, K. Nam, M. Karplus, Unsuspected pathway of the allosteric transition in hemoglobin, Proc. Natl. Acad. Sci. 108 (14) (2011) 5608–5613.